Electronic Supplementary Material (ESI) for Nanoscale.
This journal is © The Royal Society of Chemistry 2018

Ultrafast Saturable Absorption in TiS_2 Induced by Non-Equilibrium Electrons and Generation of Femtosecond Mode-Locked Laser

Xiangling Tian[a], Rongfei Wei[b], Meng Liu[c], Chunhui Zhu[d], Zhichao Luo[c], Fengqiu Wang[d], and Jianrong Qiu[a,e*]

[a]State Key Laboratory of Luminescent Materials and Devices and School of Materials Science and Engineering, South China University of Technology, Wushan Road 381, Guangzhou 510641, PR China

[b]Department of Physics, Zhejiang Normal University, Jinhua, Zhejiang, 321004, PR China

[c]School of Information and Optoelectronic Science and Engineering, South China Normal University, Guangzhou, Guangdong 510006, China

[d]School of Electronic Science and Engineering, Nanjing University, Nanjing 210093, China

[e]State Key Laboratory of Modern Optical Instrumentation, College of Materials Science and Engineering, Zhejiang University, Hangzhou, Zhejiang 310027, PR China

**qjr@zju.edu.cn*

Supporting Information

1. Light-matter interaction process

The response of materials to an optical field E is described by the material polarization P:[1]

$$P = \varepsilon_0 \left[\chi^{(1)} E + \chi^{(2)} E^2 + \chi^{(3)} E^3 + \mathrm{K} \right] \qquad \text{(S1)}.$$

Where, ε_0 and $\chi^{(s)}$ present the vacuum permittivity and the sth-order susceptibility of the material. Here, E usually consists of time-harmonic ω_n. In the weak coupling regime, only the first term in equation (S1) is important, and the material polarization P is directly proportional to the field E. Conventional optical effects, for example refraction, absorption and scattering, can be described through such a linear response. For strong fields, the higher-order (s>1) describes optical response. In second order, second-harmonic generation (SHG), sum- and difference-frequency generation, and an electro-optical response can be obtained, and only occur at surfaces in which centrosymmetry is broken. The third order contains third-harmonic generation, Kerr effect, and saturable absorption, which can occur in all materials. Since saturable absorption response is highly dependent on the complex third-order susceptibility $\chi^{(3)}$, materials with high light-matter coupling are always desirable for constructing efficient saturable absorber.

2. Methods

Materials Preparation and Characterization

Multilayer TiS_2 were prepared through liquid-phase exfoliation method. Bulk TiS_2 were first ground and then immersed into N-methyl-2-pyrrolidon (NMP) to bath ultra-ultrasonication for several hours (several consecutive 0.5 h with 0.5 h recess between them) in order to form the liquid dispersions. The initial concentration is 0.2 g/L. The stable TiS_2 dispersions were collected from the supernatant after centrifugation to remove un-exfoliated bulk matrix at 2000 rpm for 30 min. For characterization, a few droplets of the dispersion were dropped on a quartz substrate and then dried in a vacuum oven with addition of appropriate amount of ethanol to accelerate the volatilization of NMP. Before that, the quartz substrate was first subjected to hydrophilic treatment, as shown in Fig. S1. The X-ray diffraction (XRD) of multilayer TiS_2 on the quartz slide were measured using a Bruker diffractometer utilizing Cu Kα radiation (λ=1.5418 Å). Raman characterization was recorded by a confocal microscopy system (RenishaiwnVia, Gloucestershire, UK) excited at 532 nm at room temperature. The height image and spectrum were carried out using Atomic force microscopy (AFM, Nanoscope IIIa, Veeco). The optical absorption spectrum of multilayer TiS_2 on the quartz slide was measured using a Perkin-Elmer Lambda-900 UV-Vis-NIR spectrophotometer (Perkin Elmer, Waltham, MA). An empty quartz slide was used to be as reference. An X-ray photoemission spectroscopy (XPS, K-Alpha, Thermo Science, UK) was employed to characterize the binding energies of the S and Ti.

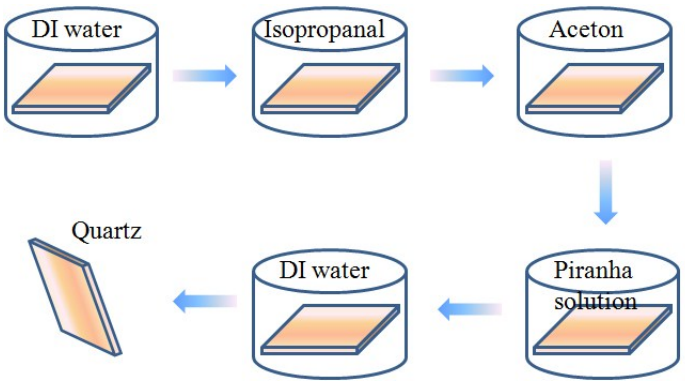

Fig. S1. The hydrophilic treatment process. The quartz substrates are first sonicated in distilled water, isopropanol and acetone for 10 min each. Then the substrates dried in nitrogen flow. After that, the dried sample was immersed in piranha solution ($30\%H_2O_2$:$98\%H_2SO_4$=3:7 in volume ratio) to etch for 10 min, then sonicated in distilled water. Finally, the substrates dried in nitrogen flow.

Nonlinear Optical Measurements

The nonlinear optical (NLO) properties were measured by Z-scan technique and more details can be found in Fig.

S1 and our previous work.[2-5] The femtosecond source was commercial Ti:sapphire (1kHz, 120 fs, and 800 nm) equipped with an optical parametric amplifier (OPA) to tune the wavelengths. A 0.5 mm thick quartz slide coated with TiS_2 was mounted on a linear translation stage which can move near the focus to imitate the change of the laser intensity. Two lenses with a focus length of 50.2 mm were used, as shown in Fig. S2. The beam waist radius is estimated to be ~24.0 μm at 1550 nm and ~12.4 μm at 800 nm. The laser intensity at the focus was monitored as I_0 measured by a dynamometer. To detect the signal changes of 800 nm, a detector (Si-biased detector, DET36A/M, 350-1100 nm, Thorlabs) was employed. Another detector based on InGaAs (DET20C/M, 800-1800 nm, Thorlabs) was used to record the changes of 1550 nm. The CS_2 solutions in standard quartz colormetric utensil were set as a criterion to evaluate the Z-scan measurement datum, with the calculated third-order nonlinear refractive index of 3.9×10^{-15} cm^2 W^{-2} which is very close to the reported value of 3.0×10^{-15} cm^2 W^{-1}.[5] This consolidates the reliability of our experimental data.

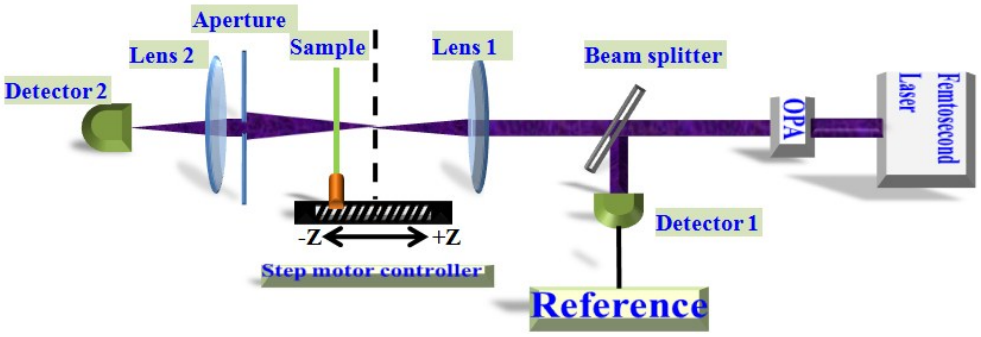

Fig. S2. Schematic illustration of Z-scan technique.

Pump-Probe Measurement

The pump-probe measurement is based on an 800 nm, 1kHz Ti:sapphire amplifier system (100 fs).[6] A wavelength of 1550 nm generated by an optical parametric amplifier (OPA) is used to excite photo-carriers in the TiS_2 and another 1550 nm light is used to probe the carriers. The pump light and the probe light were focused on the same point with the pump fluence 20 times stronger than that of the probe fluence. To detect the pump-induced change of probe, a PbSe detector (PDA20H,Thorlabs) with a lock-in amplifier (with a 500 Hz chopped pump) was employed in the pump-probe tests.

Ultrafast Pulse Generation

The pulsed laser at 1550 nm band was constructed with TiS_2 as saturable absorber in the laser cavity based on a 4 m Er-doped fiber (EDF) with a dispersion parameter of -17.3 ps/km/nm and a standard single mode fiber

(SMF). An integrated device which contains a 10/90 output coupler (OC), a polarization-independent isolator (PI-ISO) and a wavenlength division multiplexer (WDM) was used to guarantee the unidirectional operation, make the pump light couple into the cavity and output the laser. To prepare optical switch, a droplet from the stable dispersions after centrifugalization was dropped on the endface of the fiber ferrule. Then, the fiber ferrule was left into a vaccum chamber to wait for the volatilization of the solvent, just as shown in Fig. 5a. The output signal was measured by an optical spectrum analyzer (OSA, Yokagawa AQ6317C) and a high-speed real-time oscilloscope (Tektronix DSA-70804, 8GHz) equipped with a photodetector (Newport 818-BB-35F, 12.5 GHz). In addition, an autocorrelator (FR-103XL) was used to identify the corresponding pulse profile.

3. Calculation of the nonlinear optical parameter.

Briefly, the open-aperture Z-scan datum can be fitted by the nonlinear optical (NLO) model using the following equation:

$$\frac{dI(z')}{dz'} = -\alpha_0 I(z') - \beta I^2(z') \qquad \text{(S2).}$$

Here $I(z')$ represents the laser beam irradiance within the sample; z' is the propagation distance in the sample; α_0 and β are the linear absorption coefficient of the sample and the nonlinear storable absorption coefficient, respectively. Therefore the normalized transmission can be described by

$$T = \frac{1}{\sqrt{\pi}\left[\frac{\beta I_0 L_{eff}}{(1+z^2/z_0^2)}\right]} \int_{-\infty}^{+\infty} \times \ln\left[1 + \frac{\beta I_0 L_{eff}}{(1+z^2/z_0^2)} \exp(-t^2)\right] dt \qquad \text{(S3).}$$

Here T, I_0, and L represent the normalized transmittance, the peak light intensity at the focus, the thickness of the TS_2 crystals and the diffraction length of the beam, respectively. L_{eff} is the effective length of the sample and can be defined as: $L_{eff} = (1 - e^{-\alpha_0 L})/\alpha_0$. z_0 is the diffraction length of the beam following: $z_0 = \pi\omega_0^2/\lambda$, with ω_0 is the beam waist radius.

The imaginary part of the third-order nonlinear susceptibility is related to the nonlinear absorption coefficient β according to the following relation:

$$\mathrm{Im}\chi^{(3)}(\mathrm{esu}) = \frac{10^{-7} c^2 n_0^2}{96\pi^2 \omega} \beta \qquad \text{(S4).}$$

Where, c, λ, and n stand for, respectively, the speed of light in the vacuum, the wavelength of incident light, and the refractive index.

From the division of the closed-aperture Z-scan by the corresponding OA result, the NLO refractive index n_2 can be extracted from the fitting curve by the following formula:

$$T = 1 + \frac{4x\Delta\Phi}{(1+x^2)(9+x^2)} + \frac{4(3x^2-5)\Delta\Phi^2}{(1+x^2)^2(9+x^2)(25+x^2)} + \frac{32(3x^2-11)x\Delta\Phi^3}{(1+x^2)^3(9+x^2)(25+x^2)(49+x^2)} \qquad \text{(S5).}$$

Where, $\Delta\Phi = kn_2 I_0 L_{eff}$ presents the on-axis nonlinear phase shift at the focus; k is the wavelength number. Therefore the real part of the third-order nonlinear susceptibility can be extracted from the following relation:

$$\mathrm{Re}\chi^{(3)}(\mathrm{esu}) = \left[\frac{10^{-7} cn^2}{48\pi^2}\right] n_2 \qquad \text{(S6).}$$

The figure of merit (FOM) is calculated as:

$$\mathrm{FOM} = \left|\frac{\mathrm{Im}\chi^{(3)}}{\alpha_0}\right| \qquad \text{(S7).}$$

The third-order NLO susceptibility is described as:

$$\chi^{(3)} = \left[\left(\mathrm{Re}\chi^{(3)}\right)^2 + \left(\mathrm{Im}\chi^{(3)}\right)^2\right]^{1/2} \qquad \text{(S8).}$$

To determinate the saturation intensity, the non-saturable loss and the modulation depth, variation of the normalized transmittance with the input peak intensity can be fitted utilizing the equation: [7]

$$T(I) = 1 - \Delta T \cdot \exp\left(\frac{-I}{I_{sat}}\right) - T_{ns} \qquad \text{(S9),}$$

where, $T(I)$ and ΔT represent the transmittance and modutation depth; I_{sat} and T_{ns} are, respectively, the saturation intensity and the non-saturable loss. Overall, the experimental datum can be quite well fitted by choosing parameters: ΔT =49.2%/27.3%, T_{ns} =18.6%/1.90%, and I_{sat} =3.0/76.0 GW cm^{-2} at 800/1550 nm, as shown in Fig. S3.

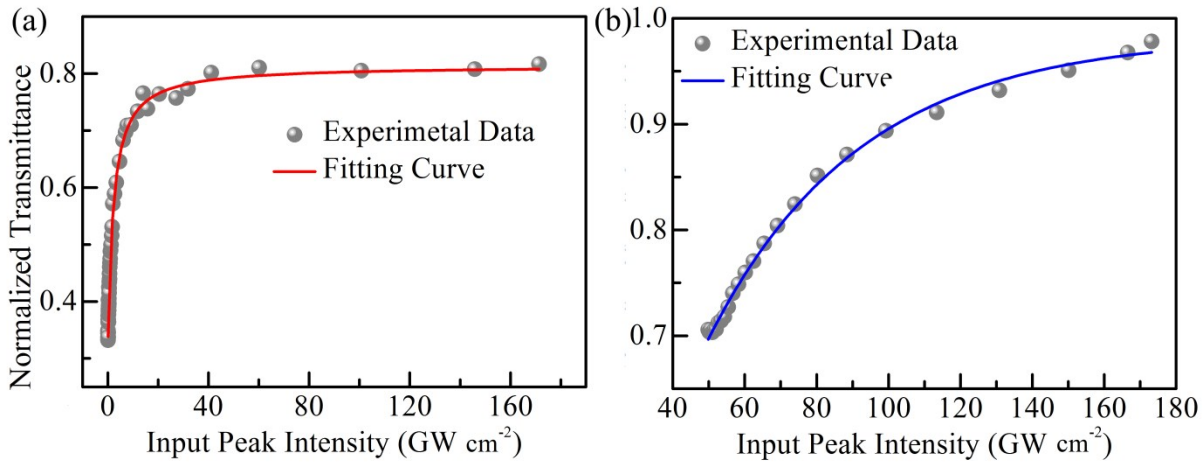

Fig. S3. Normalized transmission vs input power density at different wavelength: (a) 800 nm and (b) 1550 nm.

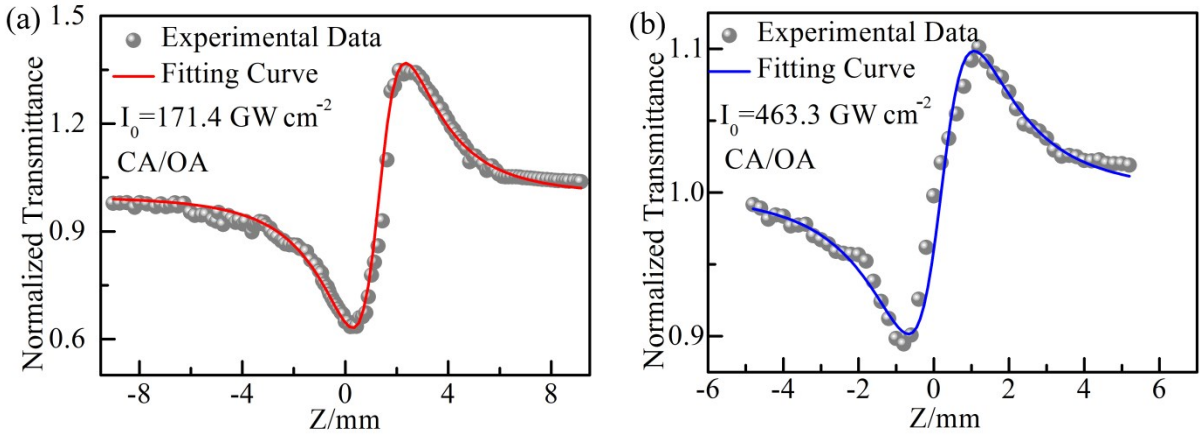

Fig. S4. CA/OA Z-scan datum of the TiS_2 under the excitation of (a) 800 nm, and (b) 1550 nm. The calculated values of the NLO refractive index n_2 are ~1.57×10^{-12} cm^2 W^{-1}, and ~1.97×10^{-13} cm^2 W^{-1}, respectively, which are larger than that of conventional NLO materials, such as Si,[8] ZnS quantum dots,[9] and ZnO quantum dots,[10] as well as one order magnitude larger than that of MoS_2, $MoSe_2$, and $MoTe_2$.[2] Subsequently, the real part of third order NLO susceptibility is calculated as ~2.11×10^{-11} esu, and ~1.967×10^{-12} esu for 800 nm and 1550 nm, respectively. Most importantly, the third order NLO susceptibility is ~3.957×10^{-11} esu and ~9.95×10^{-12} esu for 800 nm and 1550 nm, respectively, which is one order magnitude larger than that of WS_2.[2]

4. Wavelength dependent pump probe.

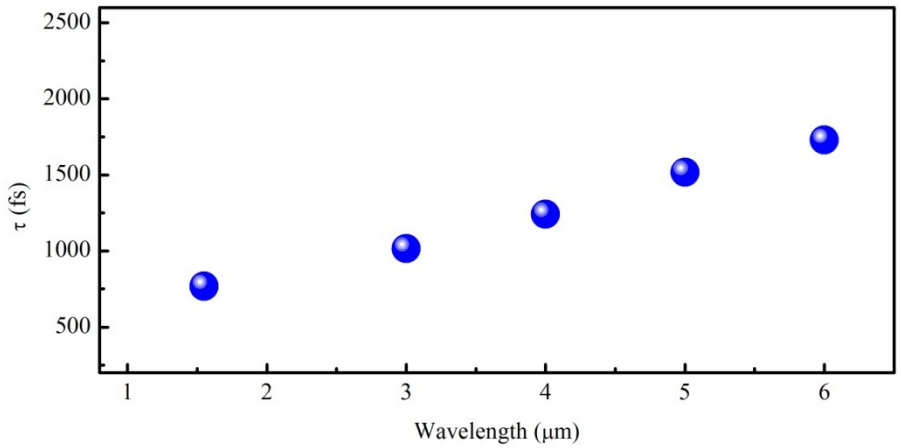

Fig. S5. Wavelength dependent pump probe measurements. The pump-probe measurement is based on an 800 nm (1kHz Ti:sapphire amplifier system 100 fs) and the probe wavelength is generated using an OPA.[6] This non-degenerated measurements provide the advantage of convenient adjustment of probe wavelength considering the ease of beam alignment (from 3.0 to 6.0 μm).[6] The recovery time is seen to slow down from 768 fs to 1728 fs as the probe wavelength was increased to 6.0 μm. In contrast to the case under the probe wavelength of 1550 nm, a single photon is not sufficient for electrons to jump from the valence band into the conduction band;[11] hence, two-photon absorption (TPA) or multi-photon absorption (MPA) is necessary and the process in Fig. 4(a) for the probe wavelength from 3.0 to 6.0 μm presents TPA or MPA. Finally, the synergy between the band structure and the non-equilibrium electrons maintains the reverse saturable absorption as well as ultrafast response.

5. RF spectrum of the mode-locked pulse.

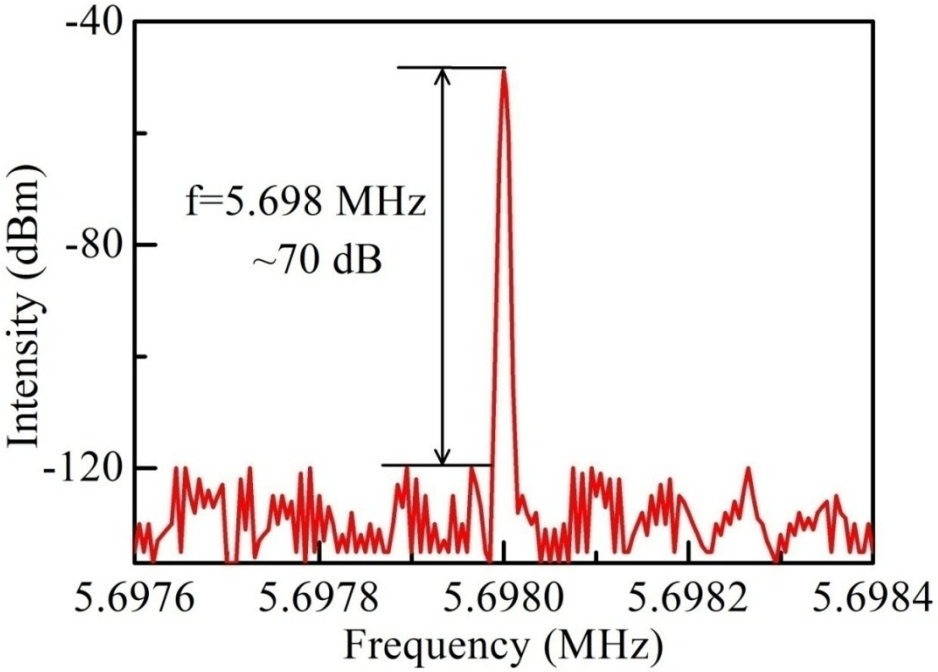

Fig. S6. Ratio-frequency (RF) spectrum indicating a stable operation with a high signal-to-noise ratio of ~70 dB (10^7 contrast). The operation frequency is related to the cavity length *L* (~35.9 m) based on the relationship of $f = c/nL$, here *c* is the light speed and *n* is the refraction index. That is to say, the frequency can be tuned by manipulating the cavity structure.

Table S1 Linear and NLO parameters of several typical saturable absorption materials

Laser	Sample	T (%)	α_0 (cm^{-1})	NLO response	β (cm GW^{-1})	Im $\chi^{(3)}$ (esu)	FOM (esu cm)	I_s (GW cm^{-2})
1030 nm, 1kHz, 340 fs	MoS_2	30.9	11.75	SA[12]	-(9.17±2.56) $\times10^{-2}$	-(6.7±1.9) $\times10^{-14}$	(5.7±1.6) $\times10^{-15}$	114±63
	$MoSe_2$	80.9	2.11	SA[12]	-(1.29±0.13) $\times10^{-2}$	-(9.4±1.0) $\times10^{-15}$	(4.22±0.27) $\times10^{-15}$	121±22
	$MoTe_2$	90.6	0.87	SA[12]	-(7.50±0.47) $\times10^{-3}$	-(5.50±0.34) $\times10^{-15}$	(6.38±0.39) $\times10^{-15}$	68±8
	Graphene	18.1	17.10	SA[12]	-(9.40±3.18) $\times10^{-2}$	-(6.9±2.3) $\times10^{-14}$	(4.03±1.36) $\times10^{-15}$	170±51
800 nm, 1kHz, 100fs	MoS_2	32.6	11.22	SA[12]	-(2.42±0.80) $\times10^{-2}$	-(1.38±0.45) $\times10^{-14}$	(1.23±0.40) $\times10^{-15}$	381±346
	$MoSe_2$	45.3	7.93	SA[12]	-(2.54±0.60) $\times10^{-3}$	-(1.45±0.34) $\times10^{-15}$	(6.9±1.6) $\times10^{-16}$	590±225
	$MoTe_2$	86.3	1.47	SA[12]	-(3.7±1.2)$\times10^{-3}$	-(2.13±0.66) $\times10^{-15}$	(1.45±0.45) $\times10^{-15}$	217±11
	Graphene	16.8	17.85	SA[12]	-(1.52±0.42) $\times10^{-2}$	-(8.7±2.4) $\times10^{-15}$	(4.9±1.4) $\times10^{-16}$	583±127
1550 nm, 35fs	Black Phosphor-us	N/A	N/A	SA[13]	-0.15$\times10^{-3}$	N/A	N/A	N/A
800 nm, 1kHz, 100 fs	Black Phosphor-us	83.1	1.85	SA[14]	-(4.08±0.11) $\times10^{-3}$	N/A	N/A	647.7±60
800 nm, 1kHz, 120 fs	TiS_2	33.7	2.68 $\times10^3$	SA[a]	-62.6	-(3.35±0.14)$\times10^{-11}$	(1.25±0.04) $\times10^{-14}$	3.0
1550 nm, 1kHz, 120 fs	TiS_2	69.5	0.86 $\times10^3$	SA[a]	-39.0	-(4.57±0.04)$\times10^{-11}$	(5.31±0.01) $\times10^{-14}$	76.0

[a]This work

References:

1. Y. Petit, S. Joly, P. Segonds, *Laser Photonics Rev.* **2013**, 7(6): 920-937.
2. R. Wei, H. Zhang, X. Tian, T. Qiao, Z. Hu, Z. Chen, X. He, Y. Yu, J. Qiu, *Nanoscale* **2016**, 8, 7704.
3. R. Wei, H. Zhang, Z. Hu, T. Qiao, X. He, Q. Guo, X. Tian, Z. Chen, J. Qiu, *Nanotechnology* **2016**, 27, 305203.
4. R. Wei, X. Tian, Z. Hu, H. Zhang, T. Qiao, X. He, Q. Chen, Z. Chen, J. Qiu, *Opt. Express* **2016**, 24, 25337.
5. R. Wei, H. Zhang, X. He, Z. Hu, X. Tian, Q. Xiao, Z. Chen, J. Qiu, *Opt. Mater. Express* **2015**, 5, 1807.
6. C. Zhu, F. Wang, Y. Meng, X. Yuan, F. Xiu, H. Luo, Y. Wang, J. Li, X. Lv, L. He, Y. Xu, J. Liu, C. Zhang, Y. Shi, R. Zhang, S. Zhu, *Nat. Commun.* **2017**, 8, 14111.
7. J. Koo, Y. I. Jhon, J. Park, J. Lee, Y. M. Jhon, J. H. Lee, *Adv. Funct. Mater.* **2016**, 26, 7454.
8. M. Dinu, F. Quochi, H. Garcia, *Appl. Phys. Lett.* **2003**, 82, 2954-2956.
9. M. Chattopadhyay, P. Kumbhakar, R. Sarkar, A. K. Mitra, *Appl. Phys. Lett.* **2009**, 95, 163115.
10. M. Chattopadhyay, P. Kumbhakar, C. S. Tiwary, A. K. Mitra, U. Chatterjee, T. Kobayashi, *Opt. Lett.* **2009**, 34, 3644-3646.
11. Y. Ge, Z. Zhu, Y. Xu, Y. Chen, S. Chen, Z. Liang, Y. Song, Y. Zou, H. Zeng, S. Xu, H. Zhang and D. Fan, *Adv. Opt. Mater.* 2018, 6, 1701166-n/a.
12. K. Wang, Y. Feng, C. Chang, J. Zhan, C. Wang, Q. Zhao, *et al. Nanoscale* **2014**, 6(18):10530-10535.
13. Y. Wang, G. Huang, H. Mu, S. Lin, J. Chen, S. Xiao, *et al. Appl. Phys. Lett.* **2015**, 107(9): 091905.
14. S.B. Lu, L.L. Miao, Z.N. Guo, X. Qi, C.J. Zhao, H. Zhang, *et al. Opt. Express* **2015**, 23(9): 11183-11194.